The Astrophysical Journal, 808:41 (6pp), 2015 July 20 doi:10.1088/0004-637X/808/1/41

FIRST DETECTION OF HCO^+ ABSORPTION IN THE MAGELLANIC SYSTEM

Claire E. Murray[1], Snežana Stanimirović[1], N. M. McClure-Griffiths[2], M. E. Putman[3], H. S. Liszt[4], Tony Wong[5], P. Richter[6,7], J. R. Dawson[8,9], John M. Dickey[10], Robert R. Lindner[1], Brian L. Babler[1], and J. R. Allison[9]

[1] Department of Astronomy, University of Wisconsin–Madison, WI 53706, USA; cmurray@astro.wisc.edu
[2] Research School for Astronomy and Astrophysics, Mount Stromlo Observatory, Cotter Road, Weston Creek, ACT 2611, Australia
[3] Department of Astronomy, Columbia University, New York, NY 10027, USA
[4] National Radio Astronomy Observatory, 520 Edgemont Road, Charlottesville, VA 22903-2475, USA
[5] Department of Astronomy, University of Illinois, 1002 West Green Street, Urbana, IL 61801, USA
[6] Institut für Physik und Astronomie, Universität Potsdam, Karl-Liebknecht-Strasse 24/25, D-14476 Potsdam-Golm, Germany
[7] Leibniz-Institut für Astrophysik Potsdam (AIP), An der Sternwarte 16, D-14482 Potsdam, Germany
[8] Department of Physics and Astronomy and MQ Research Centre in Astronomy, Astrophysics and Astrophotonics, Macquarie University, NSW 2109, Australia
[9] CSIRO Astronomy and Space Science, P.O. Box 76, Epping, NSW 1710, Australia
[10] University of Tasmania, School of Maths and Physics, Private Bag 37, Hobart, TAS 7001, Australia

Received 2015 April 27; accepted 2015 June 7; published 2015 July 16

ABSTRACT

We present the first detection of HCO^+ absorption in the Magellanic System. Using the ATCA, we observed nine extragalactic radio continuum sources behind the Magellanic System and detected HCO^+ absorption toward one source located behind the leading edge of the Magellanic Bridge. The detection is located at an LSR velocity of $v = 214.0 \pm 0.4$ km s^{-1}, with an FWHM of $\Delta v = 4.5 \pm 1.0$ km s^{-1}, and an optical depth of $\tau(HCO^+) = 0.10 \pm 0.02$. Although there is abundant neutral hydrogen (H I) surrounding the sight line in position–velocity space, at the exact location of the absorber the H I column density is low, $<10^{20}$ cm^{-2}, and there is little evidence for dust or CO emission from *Planck* observations. While the origin and survival of molecules in such a diffuse environment remain unclear, dynamical events such as H I flows and cloud collisions in this interacting system likely play an important role.

Key words: ISM: molecules – ISM: structure – Magellanic Clouds

1. INTRODUCTION

To understand galaxy evolution, which is driven by the life cycles of stars, it is necessary to investigate the origin and properties of the clouds that host star formation in a wide range of interstellar environments. The Magellanic System, including the SMC, LMC, Magellanic Bridge, Leading Arm (LA), and Magellanic Stream offer a nearby example (~50–60 kpc; Keller & Wood 2006) of an environment with interstellar conditions that sharply contrast what we find in the Milky Way (MW). In particular, the low metallicity of the Magellanic System (e.g., 10% and 45% solar metallicity, respectively, in the SMC and LMC; Rolleston et al. 2002) imply that heating and cooling mechanisms, dust-to-gas ratios, and chemical abundances may be representative of less-evolved systems at high redshift.

The Magellanic System is a complex structure that is rich in neutral hydrogen (H I; e.g., Putman et al. 2003; Stanimirović et al. 2008; Nidever et al. 2010). The LA, stretching out in front of the LMC and SMC, and the extensive, 150°-long Stream (Nidever et al. 2010) trailing behind them are understood as features of tidal (e.g., Murai & Fujimoto 1980; Yozin & Bekki 2014) and/or ram-pressure stripping (e.g., Moore & Davis 1994; Mastropietro et al. 2005) interactions between the SMC, LMC, and MW. Recent ultra-violet (UV) absorption measurements support the scenario that the Stream originated from the SMC, and observed metallicity enhancements indicate that some material has been stripped from the LMC (Fox et al. 2013, 2014; Richter et al. 2013b). There is a wealth of evidence for star formation within Magellanic structures outside the LMC and SMC, including diffuse Hα emission (e.g., Meaburn 1986), and massive, young stars in the LA (e.g., Casetti-Dinescu et al. 2014) and Bridge (e.g., Demers & Battinelli 1998), while the Stream remains starless. However, the presence and stability of cold atomic and molecular material in these extreme dynamical environments is still uncertain.

Unfortunately, molecular hydrogen (H_2), the most abundant molecule in the interstellar medium (ISM), cannot be observed directly in cold, dense environments. Many studies trace H_2 with carbon monoxide (CO), which is easily excited at low temperatures and has strong dipole-allowed rotational transitions. However, both theoretical and observational studies show that CO is less effective at self-shielding, especially at low densities (e.g., van Dishoeck & Black 1988; Sheffer et al. 2008). Therefore, the important transition regions where H_2 begins to form out of the atomic medium, are poorly traced by CO (e.g., Leroy et al. 2009). This "CO-dark" H_2 is especially prominent in low-metallicity environments where the abundance of dust grains, which provides the primary shielding mechanism for CO, is low (e.g., Wolfire et al. 2010). Accordingly, searches for Magellanic CO emission outside of the LMC and SMC have proven difficult. Following a detection of cold H I in absorption (Kobulnicky & Dickey 1999), no CO was detected in the Bridge toward source J0311–7651 (Smoker et al. 2000). Several CO clouds were detected in the Bridge just outside of the SMC (Muller et al. 2003; Mizuno et al. 2006), but these studies targeted only regions of high far-infrared excess and were very expensive in observation time.

In particular, absorption by HCO^+ appears to trace H_2 abundance in the MW (e.g., Liszt et al. 2010), and is therefore a promising tool for measuring molecular gas content and kinematics even in regions where H_2 has recently formed (Lucas & Liszt 1996). Although the thermal pressure is low in such regions, and therefore rotational transitions of molecules

are not well excited via collisions with H_2 (Lucas & Liszt 1996), absorption lines depend on column density and are therefore strong even in low excitation. There are no measurements of HCO^+ absorption in the Magellanic System, though there are two detections of H_2 in the Stream (Richter et al. 2001; Sembach et al. 2001) and one detection of H_2 in the Bridge (Lehner 2002) from FUSE far UV absorption. In addition, two sensitive searches for HCO^+ absorption in HVCs in the MW, including several Stream directions, returned only one tentative detection (Akeson & Blitz 1999; Combes & Charmandaris 2000).

In this paper, we present the results of a search for HCO^+ absorption toward nine radio continuum sources behind the Magellanic System with the ATCA. Of the nine lines of sight observed, we have one detection of HCO^+ absorption at the leading edge of the Magellanic Bridge, and eight non-detections. In Section 2, we describe the observations and data reduction, in Section 3, we analyze the data and present column density estimates, and, in Section 4, we discuss the results.

2. OBSERVATIONS

We selected our targets to be radio continuum sources located behind the Magellanic System that are bright at 3 mm. Of the nine targets, six are ATCA calibrator sources with 3 mm continuum flux densities $S_{3\,\mathrm{mm}} \geqslant 0.3$ Jy, and three are compact sources from the Australia Telescope 20 GHz Survey (AT20G) with $S_{3\,\mathrm{mm}} \geqslant 0.7$ Jy (Murphy et al. 2010).

The observations were conducted between 2014 May 28 and June 01, and additional observations were granted between 2014 July 05 and 06 due to poor initial observing conditions. We observed the HCO^+(1–0) 89.188 GHz transition with the 3 mm receivers on the ATCA in the EW 352 m configuration, which corresponds to a $\sim 2''$ synthesized beam. We used the CFB 64 M-32k correlator mode to cover the velocity[11] range from $180-360$ km s^{-1} within a single zoom-band. Given that all sources are compact and bright, the target sources performed as their own phase calibrators. The ATCA calibrators 0537–441 and 1921–293 were observed once every 30 minutes for bandpass calibration, Uranus was observed for 30 minutes at the end of each session for flux calibration, and pointing was corrected on each target every 20 minutes.

All data were reduced using standard packages in MIRIAD (Sault et al. 1995). Following flagging and calibration, spectral line cubes were constructed using the task INVERT with uniform weighting and 0.2 km s^{-1} velocity resolution. Final, cleaned image cubes were produced following 1000 minor iterations in CLEAN, and all sources were unresolved. The cubes were Hanning-smoothed to 0.8 km s^{-1} resolution within MIRIAD. We then extracted the HCO^+ spectrum from the central pixel of each cube[12] and calculated the absorption spectrum, $\exp(\tau(HCO^+))$, by dividing the line by the source continuum.

Table 1 includes position and flux information for the nine observed sources. These include: (1) source name, (2–3) R.A. and decl. (J2000), (4–5) Galactic latitude and longitude (°), (6) measured continuum flux density at 3 mm (Jy), (7) total on-source integration time (hr), (8) rms noise in HCO^+ optical depth, per 0.8 km s^{-1} channel, and (9) source type.

[11] All velocities quoted in this paper are in the kinematic or standard LSR frame.

[12] The results are consistent with extracting the spectra directly from the UV data.

3. ANALYSIS

3.1. Spectral Line Fitting

To search for absorption signatures in the observed HCO^+ spectra, we used the Bayesian analysis technique developed, implemented, and described by Allison et al. (2012). Given a likelihood function and prior distribution, this procedure searches all parameter space using the MULTINEST Monte Carlo sampling algorithm (Feroz & Hobson 2008) and calculates the resulting posterior probability distribution and evidence statistic. For this study, we tested for the presence of a single Gaussian function in each unsmoothed HCO^+ absorption spectrum given the following priors: (1) the line width is not less than the channel spacing (0.2 km s^{-1}) or greater than the bandwidth (180 km s^{-1}); (2) the spectral noise is equal to the standard deviation in off-line channels; (3) the spectral channels are independent. We considered an absorption line to be "detected" if the Bayesian evidence statistic of the Gaussian model is greater than the evidence statistic for a model containing no spectral lines.

After analyzing all spectra, we detected one absorption line in the spectrum toward J0454–810. We display the J0454–810 spectrum with the Gaussian model in the top panel of Figure 1. The detection significance is described by $R = 7$, where R is the natural logarithm of the Bayesian evidence statistic for the Gaussian model divided by evidence statistic for a model containing only noise. The line is located at $v = 214.0 \pm 0.4$ km s^{-1}, has an FWHM of $\Delta v = 4.5 \pm 1.0$ km s^{-1}, and an optical depth of $\tau(HCO^+) = 0.10 \pm 0.02$. The integrated optical depth of the line derived from the model is, $\int \tau(HCO^+) dv = 0.44 \pm 0.08$, which indicates a $\sim 5\sigma$ detection significance and is consistent with the quoted R value.

As a sanity check, we note that the detected HCO^+ absorption line is present in the J0454–810 spectrum for: (1) each of the four individual days of observations, (2) both 0.2 and 0.8 km s^{-1} velocity resolutions, (3) data reduced using different subsets of the available ATCA antennas, and (4) both linear polarizations. We are therefore confident that the feature is not spurious.

3.2. Column Densities

Assuming excitation in equilibrium with the cosmic microwave background (Lucas & Liszt 1996), we calculated the HCO^+ column density, $N(HCO^+)$, from the $J = 1$–0 optical depth ($\tau(HCO^+)$) for an HCO^+ dipole moment of 3.92 Debye (Mount et al. 2012), so that,

$$N\left(\mathrm{HCO^+}\right) = 1.107 \times 10^{12}\ \mathrm{cm^{-2}} \int \tau\left(\mathrm{HCO^+}\right)(v) dv, \quad (1)$$

where the line integral is expressed in km s^{-1}.

For the J0454–810 detection, we integrated the Gaussian model to compute $N(HCO^+)$ using Equation (1). For the non-detection sight lines, we computed a limit to $N(HCO^+)$ using a 3σ upper limit to $\tau(HCO^+)$ (with $\sigma_{\tau(HCO^+)}$ in Table 1) and assumed a line width of 4.5 km s^{-1} based on the J0454–810 detection.

From MW studies, there is a correlation between $N(HCO^+)$ and $N(H_2)$, given by $X(HCO^+) = N(HCO^+)/N(H_2) \sim$

Table 1
Source Information

Source	R.A. (J2000) (hh:mm:ss)	Decl. (J2000) (dd:mm:ss)	l (°)	b (°)	$S_{3\,mm}$ (Jy)	Time (hr)	$\sigma_{\tau(HCO^+)}$ (per 0.8 km s^{-1})[a]	Type[b]
J0056–572	00:58:46.6	–56:59:11.5	300.926	–60.113	0.9	2.7	0.059	···
J0102–7546	01:02:18.8	–75:46:53.0	302.043	–41.328	0.6	1.7	0.090	AT20G
J0208–512	02:10:46.2	–51:01:01.9	276.102	–61.778	2.1	2.3	0.051	···
J0311–7651	03:11:55.3	–76:51:51.0	293.440	–37.553	0.8	2.3	0.054	AT20G
J0440–6952	04:40:47.8	–69:52:18.1	281.836	–36.399	0.6	4.0	0.046	···
J0454–810	04:50:05.4	–81:01:02.2	293.851	–31.371	1.5	3.3	0.026	···
J0506–6109	05:06:44.0	–61:09:41.0	270.550	–36.072	0.4	1.7	0.090	AT20G
J0530–727	05:29:30.0	–72:45:28.5	283.850	–31.857	0.8	3.3	0.019	···
J0637–752	06:35:46.5	–75:16:16.8	286.368	–27.158	1.8	2.8	0.010	···

Notes.
[a] rms noise in $\tau(HCO^+)$ per 0.8 km s^{-1} channel.
[b] ATCA calibrators unless indicated as AT20G sources from Murphy et al. (2010).

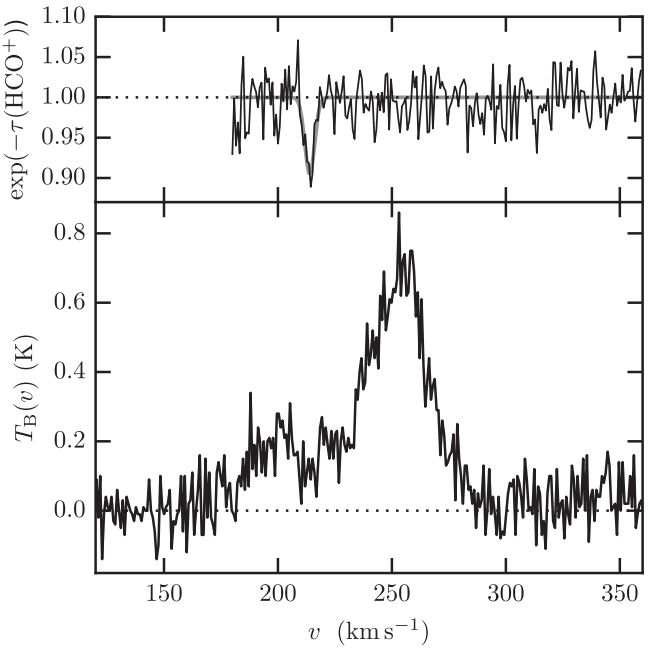

Figure 1. Top: ATCA HCO^+ absorption spectrum ($\tau(HCO^+)$) toward J0454–810. The Gaussian model obtained using Bayesian analysis (Section 3) is overlaid in gray. Bottom: H I brightness temperature spectrum ($T_B(v)$) in the direction of J0454–810 from GASS (McClure-Griffiths et al. 2009). Two peaks appear in H I emission ($v \sim 200$, 260 km s^{-1}), offset from the detected HCO^+ absorption ($v = 214.0 \pm 0.4$ km s^{-1}).

2×10^{-9} (e.g., Liszt et al. 2010). Although the correlation may be different in the lower-metallicity Magellanic System, we applied this factor to $N(HCO^+)$ to estimate the Magellanic H_2 column density, $N(H_2)_{Mag}$.

In addition, we extracted H I emission spectra from the stray radiation-corrected Galactic All Sky Survey (GASS; McClure-Griffiths et al. 2009; Kalberla et al. 2010) for each line of sight. From these data, we computed $N(H\,I)_{Mag}$, assuming that the H I is optically thin:

$$N(H\,I)_{Mag} = C_0 \int_{180}^{360} T_B(v)dv, \quad (2)$$

where $C_0 = 1.823 \times 10^{18}$ cm^{-2} K^{-1}(km s^{-1})$^{-1}$ and $T_B(v)$ (K) is the H I brightness temperature integrated between radial velocities: $180 \leqslant v \leqslant 360$ km s^{-1}. All column densities described above are included in Table 2.

Table 2
Column Densities and Limits

Source	$N(H\,I)_{Mag}$ (10^{20} cm^{-2})	$N(HCO^+)$ (10^{12} cm^{-2})[a]	$N(H_2)_{Mag}$ (10^{20} cm^{-2})[b]
J0056–572	0.02 ± 0.01	⩽0.88	⩽4.4
J0102–7546	0.21 ± 0.03	⩽1.34	⩽6.7
J0208–512	0.05 ± 0.02	⩽0.76	⩽3.8
J0311–7651	0.92 ± 0.02	⩽0.81	⩽4.1
J0440–6952	1.00 ± 0.02	⩽0.68	⩽3.4
J0454–810	0.42 ± 0.03	0.49 ± 0.09	2.45 ± 0.45
J0506–6109	0.01 ± 0.02	⩽1.34	⩽6.7
J0530–727	7.17 ± 0.03	⩽0.28	⩽1.4
J0637–752	0.13 ± 0.03	⩽0.15	⩽0.8

Notes.
[a] Assuming 4.5 km s^{-1} line width.
[b] Based on $N(HCO^+)$ and $X(HCO^+) = 2 \times 10^{-9}$.

3.3. Estimating Dust, H_2 and CO from Planck

Using available *Planck* maps (version 1.20) and H I emission from GASS, we can estimate limits to the Magellanic dust reddening, H_2 column density, and CO brightness along each line of sight.

To correct for the Galactic contribution, we computed the total Galactic H I column density, $N(H\,I)_{MW}$, by integrating the GASS $T_B(v)$ profile in Equation (2) for all $v \leqslant 180$ km s^{-1}. We then converted this column density to an estimate of the reddening due to the MW, $E(B-V)_{MW}$, using the results from Liszt (2014): $E(B-V)_{MW} = N(H\,I)_{MW}/8.3 \times 10^{21}$ cm^{-2} mag^{-1}, which holds for $E(B-V) < 0.3$ mag. To find the total reddening along the line of sight, $E(B-V)_{tot}$, we used the *Planck* model of dust radiance, or total dust emission integrated over frequency, $\mathcal{R}$. The Planck collaboration showed that $\mathcal{R}$ is a better tracer of the total column density than 353 GHz dust optical depth in diffuse, high-latitude regions, and exhibits the strong correlation: $E(B-V)/\mathcal{R} = (5.40 \pm 0.09) \times 10^5$ (Planck Collaboration et al. 2014). We used this correlation to compute $E(B-V)_{tot}$, and then subtracted $E(B-V)_{MW}$ from $E(B-V)_{tot}$ to estimate the total Magellanic contribution,

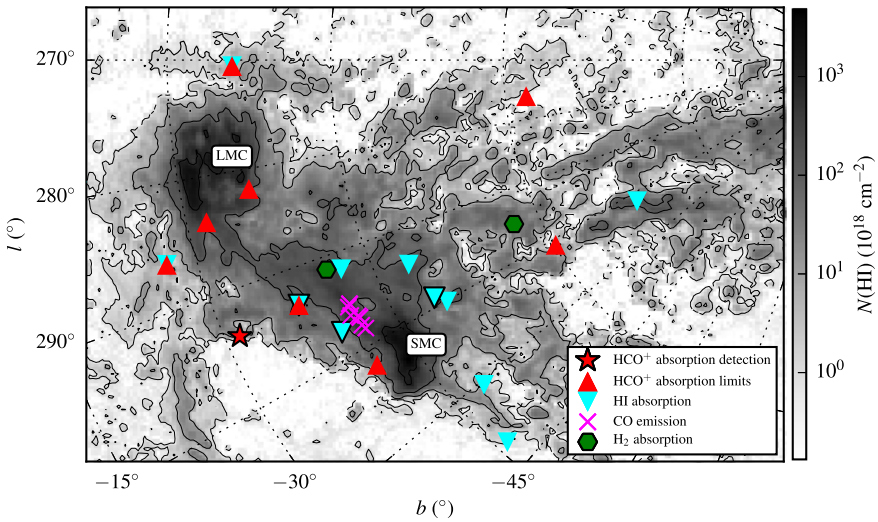

Figure 2. Positions of the ATCA HCO^+ absorption detection (red star) and limits (red triangles) overlaid on an $N(H\,I)$ map of the Magellanic System from Putman et al. (2003), where the contours correspond to (1, 10, 100, 1000) $\times$ 10^{18} cm^{-2}. We overlay H I absorption (Kobulnicky & Dickey 1999; Matthews et al. 2009), CO emission (Muller et al. 2003; Mizuno et al. 2006), and H_2 absorption (Richter et al. 2001; Lehner 2002) outside the LMC and SMC. Detections are distinguished from limits by solid black symbol outlines.

$E(B-V)_{Mag}$. For all lines of sight, we find $E(B-V)_{Mag} \sim 0.001-0.01$ mag.

We note that the above calculations require the assumption that the dust-to-gas ratio is constant across the sampled volume. Using results from FUSE observations of the SMC and LMC, we converted $E(B-V)_{Mag}$ to another estimate of $N(H_2)_{Mag}$ given $N(H_2)/E_{B-V} = 6 \times 10^{20}$ cm^{-2} mag^{-1} (Welty et al. 2012). For all lines of sight, we find $N(H_2)_{Mag} \sim 10^{17}-10^{18}$ cm^{-2}. Finally, we estimated the Magellanic CO brightness, $W_{CO,Mag} = N(H_2)_{Mag}/X_{CO,Mag}$, by assuming (from observations of the SMC): $X_{CO,Mag} = 4 \times 10^{21}$ $cm^{-2}(K\ km\ s^{-1})^{-1}$ (e.g., Bolatto et al. 2013). For all lines of sight, we find $W_{CO,Mag} \sim 10^{-3}-10^{-4}$ K km s^{-1}.

4. DISCUSSION

4.1. Comparisons with Previous Work

The HCO^+ absorption detection toward J0454–810 is the first of its kind in the Magellanic System, and suggests the presence of molecular gas far outside of the SMC and LMC. Of the eight non-detections, only two were more sensitive and six were up to three times less sensitive due to compromised weather conditions. Overall, our ATCA observations are more sensitive than previous searches for HCO^+ absorption in diffuse, high-velocity clouds. These previous studies had typical 3σ limits to an HCO^+ optical depth of $\sim$0.1–0.9 per 0.6 km s^{-1} channels and returned no detections (Akeson & Blitz 1999) and one tentative and non-confirmed detection (Combes & Charmandaris 2000) in clouds with $N(H\,I) < 10^{20}$ cm^{-2}.

Our detected absorption line is wider ($\Delta v = 4.5 \pm 1.0$ km s^{-1}) than individual HCO^+ absorption lines detected in the MW ($\Delta v \sim 1-2$ km s^{-1}; Lucas & Liszt 1996), and the only previously reported high-velocity cloud detection ($\Delta v = 1.1$ km s^{-1}; Combes & Charmandaris 2000). Although our measured Magellanic column density, $N(HCO^+) = (0.49 \pm 0.09) \times 10^{12}$ cm^{-2}, is slightly smaller than the typical column densities observed in the MW ($\sim 1-10 \times 10^{12}$ cm^{-2}; Lucas & Liszt 1996), it is similar to those observed in diffuse regions. For example, for the only sight line with $N(H\,I) \sim 10^{20}$ cm^{-2}, Liszt et al. (2010) measure $N(HCO^+) = (0.25 \pm 0.08) \times 10^{12}$ cm^{-2}.

In Figure 2, we overlay the observed HCO^+ absorption coordinates on an $N(H\,I)$ image of the Magellanic System from the Parkes radio telescope (Putman et al. 2003). The detection is located at the leading edge of the Magellanic Bridge. Nearby regions contain other evidence for cold atomic and molecular gas, including H I detected in absorption with temperatures $\sim$20–70 K (Kobulnicky & Dickey 1999; Matthews et al. 2009), and CO emission close to the SMC (Muller et al. 2003; Mizuno et al. 2006). However, the detected HCO^+ absorption probes molecular gas farther away from the LMC and SMC (about 10 kpc from the SMC's center) than any previous radio or millimeter-wave studies.

Our estimates of $N(H_2)_{Mag}$ in Table 2 ($\sim 10^{20}$ cm^{-2}) are orders of magnitude higher than both the *Planck* based estimates ($\sim 10^{17-18}$ cm^{-2}) and those from FUSE UV-absorption in the Stream and Bridge. Toward Fairall 9, located at the beginning of the Stream in a region of enhanced metallicity likely stripped from the LMC, Richter et al. (2013b) measured $\log(N(H_2)_{Mag}) = 17.93^{+0.19}_{-0.16}$ cm^{-2}. Toward an early-type star in the Bridge, Lehner (2002) measured $\log(N(H_2)_{Mag}) \approx 15.4$ cm^{-2}. The discrepancies between these values and our Table 2 estimates suggest that the that the MW-based conversion factor $X(HCO^+)$ may not be applicable in the lower-metallicity Magellanic regime. Given that the $X(CO)$ factor is expected to be up to a factor of 100 higher in low-metallicity regimes (e.g., Bolatto et al. 2013), it is likely that $X(HCO^+)$ will be similarly different in the Magellanic system. Additional measurements of HCO^+ and H_2 column densities are required to constrain this value further.

4.2. Origin of the Detected HCO^+

The origin and survival of the detected HCO^+ in the highly diffuse ($N(\mathrm{H\,I}) = (0.42 \pm 0.03) \times 10^{20}\,\mathrm{cm^{-2}}$) region of the Bridge is puzzling. The material either formed within the Bridge or it originated from a stripping interaction with the LMC or, more likely given its proximity, the SMC. The age of the Bridge is constrained to 100–300 Myr by the oldest detected stellar populations known to have formed in situ (e.g., Harris 2007). Within the Bridge, low metallicities (~0.05 Solar; Lehner et al. 2008) indicate reduced dust grain formation rates, and young stellar populations (e.g., Demers & Battinelli 1998) indicate potentially strong UV radiation fields (10–100 × MW value). These two properties, as discussed by Lehner (2002), imply that molecule formation and destruction equilibrium cannot be reached within the Bridge's lifetime for reasonable hydrogen volume densities (e.g., $n_{\mathrm{H}} \leqslant 100\,\mathrm{cm^{-3}}$; Lehner 2002). Therefore, extremely high densities ($n_{\mathrm{H}} \gg 100\,\mathrm{cm^{-3}}$) are likely required in the Bridge for equilibrium molecule formation to occur. This was also discussed by Kobulnicky & Dickey (1999) in the context of cold atomic gas formation in the Bridge.

However, non-equilibrium molecule formation may be responsible. Simulations show that ram-pressure effects during the SMC–LMC interaction which created the Bridge (required to explain the Bridge's observed in situ star formation; e.g., Connors et al. 2006; Besla et al. 2012) can produce high-density, star formation-ready peaks within the diffuse medium (e.g., Mastropietro et al. 2009). Further simulations of ram pressure-stripping of the ISM from galaxies have shown that stars can form within diffuse, gaseous tails when ablated gas cools and condenses in the turbulent wake of the stripping interaction (e.g., Tonnesen & Bryan 2012). In the bottom panel of Figure 1, we display the H I brightness temperature spectrum from GASS (McClure-Griffiths et al. 2009). There is an offset between the two peaks in H I and the location of HCO^+ absorption, which may be indicative of a shock driven by dynamical interactions and support for molecule formation in the post-shock material.

In terms of molecule survival in this environment, dust is very important, as it provides shielding against the UV radiation field and acts as a catalyst for grain formation. Our *Planck*-based estimates indicate very little dust and CO along the lines of sight probed by this study. A lack of shielding by dust or sufficiently large $N(\mathrm{H\,I})$ means that the molecular material identified by the HCO^+ detection must disperse quickly and we may be observing the material in the process of being disrupted.

Alternatively, the detection presented here may not be tracing dense molecular gas. Comprehensive studies using the Plateau de Bure Interferometer (e.g., Lucas & Liszt 1996; Liszt et al. 2010) have shown that strong absorption by HCO^+, ^{12}CO, CN, HCN, HNC, and C_2H can be found in surprisingly diffuse MW regions ($A_V < 1$ mag) where fully developed molecular chemistry is not expected to exist. Recent *Herschel Space Observatory* observations have detected similar molecular species to HCO^+, including OH^+, in extremely diffuse gas where the fraction of H_2 is <5% (Indriolo et al. 2015). These studies indicate that many diatomic and polyatomic molecules can form and reach significant abundances even when they are not well-shielded.

In support of this scenario, there is a growing supply of evidence for the existence of molecules and star formation in H I-diffuse, dust-poor structures. For example, low-$N(\mathrm{H\,I})$ intermediate-velocity clouds in the MW halo exhibit ubiquitous H_2 absorption (Richter et al. 2003b, 2003a). Widespread CO emission has been detected in the ram pressure-stripped tail of the Norma cluster galaxy ESO 137–001, 40 kpc away from the disk (Jáchym et al. 2014). In addition, young stellar associations in low-$N(\mathrm{H\,I})$ regions ($\sim 10^{20}\,\mathrm{cm^{-2}}$) with high H I velocity dispersions ($\sim 30\,\mathrm{km\,s^{-1}}$) have been detected in stripped tails up to 30 kpc away from NGC 1533 (Werk et al. 2008).

Overall, additional observations of molecular gas tracers at high sensitivity and in a wide range of galactic environments are needed to understand the formation and evolution of molecular gas at these extremes. HCO^+ absorption is a promising tracer of this material, and future observations with ALMA will be able to confirm the detection presented here and extend the sample of available sources to probe the full extent of the Magellanic System and the outskirts of galaxies at higher redshifts.

5. SUMMARY

Using the ATCA, we detected HCO^+ absorption in the Magellanic System for the first time. We observed nine background continuum sources, and detected one absorption line toward J0454–810, with an HCO^+ column density of $N(HCO^+) = (0.49 \pm 0.09) \times 10^{12}\,\mathrm{cm^{-2}}$. The detection is located in a diffuse (H I column density of $N(\mathrm{H\,I}) < 10^{20}\,\mathrm{cm^{-2}}$) region at the leading edge of the Magellanic Bridge, where there is little current evidence for either dust or CO emission based on *Planck* and GASS H I observations. Despite the low $N(\mathrm{H\,I})$, this molecular material may have formed as part of a dynamical interaction during the evolution of the Bridge. Ultimately, higher-sensitivity searches for HCO^+ absorption and other molecular gas tracers across the Magellanic System are strongly needed to better understand the formation history and star formation potential of this complex, low-metallicity structure.

This work was supported by the National Science Foundation (NSF) Early Career Development (CAREER) Award AST-1056780. C.E.M. acknowledges support by the NSF Graduate Research Fellowship and the Wisconsin Space Grant Institution. We thank the scheduling team at the Australia Telescope Compact Array (ATCA) for granting additional observing time. The ATCA is part of the Australia Telescope National Facility, which is funded by the Commonwealth of Australia for operation as a National Facility managed by CSIRO. The National Radio Astronomy Observatory is operated by Associated Universities, Inc., under contract with the NSF.

REFERENCES

Akeson, R. L., & Blitz, L. 1999, ApJ, 523, 163
Allison, J. R., Sadler, E. M., & Whiting, M. T. 2012, PASA, 29, 221
Besla, G., Kallivayalil, N., Hernquist, L., et al. 2012, MNRAS, 421, 2109
Bolatto, A. D., Wolfire, M., & Leroy, A. K. 2013, ARA&A, 51, 207
Casetti-Dinescu, D. I., Moni Bidin, C., Girard, T. M., et al. 2014, ApJL, 784, LL37
Combes, F., & Charmandaris, V. 2000, A&A, 357, 75
Connors, T. W., Kawata, D., & Gibson, B. K. 2006, MNRAS, 371, 108
Demers, S., & Battinelli, P. 1998, AJ, 115, 154
Feroz, F., & Hobson, M. P. 2008, MNRAS, 384, 449
Fox, A. J., Richter, P., Wakker, B. P., et al. 2013, ApJ, 772, 110

Fox, A. J., Wakker, B. P., Barger, K. A., et al. 2014, ApJ, 787, 147
Harris, J. 2007, ApJ, 658, 345
Indriolo, N., Neufeld, D. A., Gerin, M., et al. 2015, ApJ, 800, 40
Jáchym, P., Combes, F., Cortese, L., Sun, M., & Kenney, J. D. P. 2014, ApJ, 792, 11
Kalberla, P. M. W., McClure-Griffiths, N. M., Pisano, D. J., et al. 2010, A&A, 521, AA17
Keller, S. C., & Wood, P. R. 2006, ApJ, 642, 834
Kobulnicky, H. A., & Dickey, J. M. 1999, AJ, 117, 908
Lehner, N. 2002, ApJ, 578, 126
Lehner, N., Howk, J. C., Keenan, F. P., & Smoker, J. V. 2008, ApJ, 678, 219
Leroy, A. K., Bolatto, A., Bot, C., et al. 2009, ApJ, 702, 352
Liszt, H. 2014a, ApJ, 780, 10
Liszt, H. S., Pety, J., & Lucas, R. 2010, A&A, 518, AA45
Lucas, R., & Liszt, H. 1996, A&A, 307, 237
Matthews, D., Staveley-Smith, L., Dyson, P., & Muller, E. 2009, ApJL, 691, L115
Mastropietro, C., Burkert, A., & Moore, B. 2009, MNRAS, 399, 2004
Mastropietro, C., Moore, B., Mayer, L., Wadsley, J., & Stadel, J. 2005, MNRAS, 363, 509
McClure-Griffiths, N. M., Pisano, D. J., Calabretta, M. R., et al. 2009, ApJS, 181, 398
Meaburn, J. 1986, MNRAS, 223, 317
Mizuno, N., Muller, E., Maeda, H., et al. 2006, ApJL, 643, L107
Moore, B., & Davis, M. 1994, MNRAS, 270, 209
Mount, B. J., Redshaw, M., & Myers, E. G. 2012, PhRvA, 85, 012519
Muller, E., Staveley-Smith, L., & Zealey, W. J. 2003, MNRAS, 338, 609
Murai, T., & Fujimoto, M. 1980, PASJ, 32, 581
Murphy, T., Sadler, E. M., Ekers, R. D., et al. 2010, MNRAS, 402, 2403
Nidever, D. L., Majewski, S. R., Butler Burton, W., & Nigra, L. 2010, ApJ, 723, 1618
Planck Collaboration, Abergel, A., Ade, P. A. R., et al. 2014, A&A, 571, AA11
Putman, M. E., Staveley-Smith, L., Freeman, K. C., Gibson, B. K., & Barnes, D. G. 2003, ApJ, 586, 170
Richter, P., Fox, A. J., Wakker, B. P., et al. 2013, ApJ, 772, 111
Richter, P., Sembach, K. R., & Howk, J. C. 2003a, A&A, 405, 1013
Richter, P., Sembach, K. R., Wakker, B. P., & Savage, B. D. 2001, ApJL, 562, L181
Richter, P., Wakker, B. P., Savage, B. D., & Sembach, K. R. 2003b, ApJ, 586, 230
Rolleston, W. R. J., Trundle, C., & Dufton, P. L. 2002, A&A, 396, 53
Sault, R. J., Teuben, P. J., & Wright, M. C. H. 1995, in ASP Conf. Ser. 77, Astronomical Data Analysis Software and Systems IV, ed. R. A. Shaw, H. E. Payne, & J. J. E. Hayes (San Francisco, CA: ASP)
Sembach, K. R., Howk, J. C., Savage, B. D., & Shull, J. M. 2001, AJ, 121, 992
Sheffer, Y., Rogers, M., Federman, S. R., et al. 2008, ApJ, 687, 1075
Smoker, J. V., Keenan, F. P., Polatidis, A. G., et al. 2000, A&A, 363, 451
Stanimirović, S., Hoffman, S., Heiles, C., et al. 2008, ApJ, 680, 276
Tonnesen, S., & Bryan, G. L. 2012, MNRAS, 422, 1609
van Dishoeck, E. F., & Black, J. H. 1988, ApJ, 334, 771
Welty, D. E., Xue, R., & Wong, T. 2012, ApJ, 745, 173
Werk, J. K., Putman, M. E., Meurer, G. R., et al. 2008, ApJ, 678, 888
Wolfire, M. G., Hollenbach, D., & McKee, C. F. 2010, ApJ, 716, 1191
Yozin, C., & Bekki, K. 2014, MNRAS, 443, 522